

## THICKNESS-INDEPENDENT COMPLEX PERMITTIVITY DETERMINATION OF PARTIALLY FILLED THIN DIELECTRIC MATERIALS INTO RECTANGULAR WAVEGUIDES

U. C. Hasar <sup>†</sup>

Department of Electrical and Electronics Engineering  
Ataturk University  
Erzurum 25240, Turkey

**Abstract**—A microwave method has been proposed for accurate complex permittivity measurement of thin dielectric materials partially filling the waveguide. The method employs propagation constant measurements at two locations of the sample inside its holder. It increases the accuracy of permittivity measurements of similar methods in the literature since it utilizes the measurements of the distances between the inner waveguide walls and sample lateral surfaces instead of directly measuring the sample thickness. It has been validated by comparing the measured complex permittivity of a thin Plexiglas sample by the proposed method with that of the method in the literature.

### 1. INTRODUCTION

Microwave engineering requires precise knowledge of electromagnetic properties of materials at microwave frequencies since microwave communications are playing more and more important roles in military, industrial, and civilian life [1–3]. Various microwave techniques have been proposed to determine these properties of material under test [1–20]. These methods can be divided into two groups as a) resonant and b) nonresonant methods [1]. Resonant methods have much better accuracy and sensitivity than nonresonant methods [1] and are generally applied to characterization of low-loss materials. On the other hand, nonresonant methods have relatively higher accuracy

---

Corresponding author: U. C. Hasar (ugurcem@atauni.edu.tr).

<sup>†</sup> Also with Department of Electrical and Computer Engineering, Binghamton University, Binghamton, NY 13902, USA.

over a broad frequency band and necessitate less sample preparation compared to resonant methods. Additionally, they allow the frequency-domain or time-domain analysis, or both.

Electrical characterization of thin materials is needed for several reasons. For instance, the dielectric constant of vegetation has a direct effect on radar backscatter measured by airborne and space-borne microwave sensors. A good understanding of the dielectric properties of vegetation leaves is vital for extraction of useful information from the remotely sensed data for earth resources monitoring and management [17]. Also, in the field of electronics, it has been a lasting key issue to evaluate the relative complex permittivity ( $\epsilon_r$ ) of thin dielectric materials such as high-density packaging (HDP) [18].

Permittivity measurements of thin materials can be performed by using non-destructive methods such as open-ended waveguide and coaxial methods [4]. In order to accurately measure the  $\epsilon_r$  for these methods, samples with larger apertures should be prepared. Besides, the sample must be sufficiently thick so that the interaction of the electromagnetic field with the non-contacting boundaries or sample holder is negligible [15]. Furthermore, any bad contact present between the waveguide or coaxial aperture and the sample surface may degrade the accuracy of measurements [20]. Finally, for open-ended waveguides and coaxial probes with a lift-off distance, thin samples may sag and thus alter the theoretical computations [21].

The transmission-reflection nonresonant methods are the most commonly used methods due to their simplicity and broadband frequency coverage [1, 6–20]. When applying these methods for measurements of thin materials, various approaches have been proposed. Although some of these methods are attractive in determining accurate permittivity, they require that the sample be precisely fitted into the waveguide aperture [6–13, 17–19]. In some instances, the presence of air gaps between sample surfaces and inner waveguide walls may procedure higher order modes or decrease the accuracy and performance of the proposed technique [14–16]. A promising solution to this problem is to partially fill the sample inside the waveguide aperture. Recently, different techniques have been proposed for permittivity determination using this approach [14–16, 19]. While the methods in [14, 15, 19] are suitable for thin and moderately thin solid materials, that in [16] especially designed for the  $\epsilon_r$  measurement of liquid materials sandwiched by two plugs. In [14, 15, 19], it is assumed that the sample is located at the center of the longer section of the waveguide aperture to simplify the expressions. However, any shift from the center of the longer section of the waveguide may decrease the accuracy and performance of

measurements since these methods depend on the assumption that the sample is located at the center of the waveguide. In addition, these methods require precise knowledge on the length of the sample for accurate measurements. The accuracy may lower for thin samples since the accuracy of thickness measurements of these samples significantly decreases with a decrease in their lengths. Therefore, any method which eliminates the dependency of sample length on  $\varepsilon_r$  measurements will be helpful in partially loaded waveguides. In this research paper, we propose a simple and feasible technique to circumvent the need for sample thickness information in  $\varepsilon_r$  measurement of thin samples in partially filled waveguides.

## 2. THEORETICAL BACKGROUND

The problem under investigation is depicted in Fig. 1. In this figure, the thin dielectric sample with a length of  $L$  partially filling the waveguide aperture is asymmetrically located into the waveguide for its permittivity determination. For region II in Fig. 1, either transverse electric to  $+z$ -direction ( $TE^z$ ) modes or transverse magnetic to  $z$ -direction ( $TM^z$ ) modes cannot satisfy the boundary conditions individually [22]. In this region, field configurations that are combinations of  $TE^z$  and  $TM^z$  modes can be solutions and satisfy the boundary conditions of such a partially filled waveguide [22, 23].

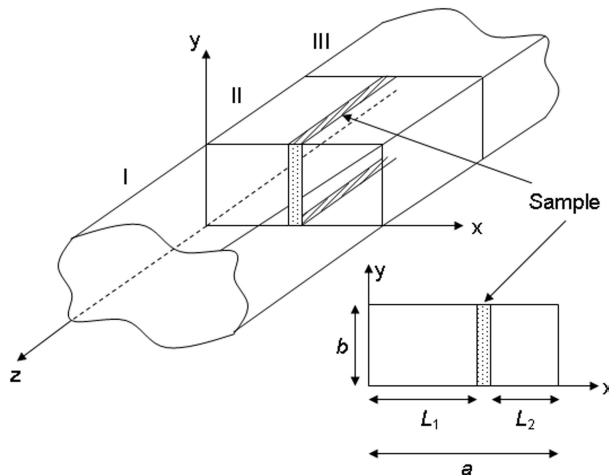


**Figure 1.** Complex permittivity determination of a thin sample with length  $L$  asymmetrically partially filling the waveguide aperture.

In general, in region II, the  $\varepsilon_r$  is a function of transverse electric to  $x$ -direction (TE <sup>$x$</sup>  or longitudinal section electric to  $x$ -direction-LSE <sup>$x$</sup> ) and transverse magnetic to  $x$ -direction (TM <sup>$x$</sup>  or longitudinal section magnetic to  $x$ -direction-LSM <sup>$x$</sup> ) modes [22, 24]. Electric and magnetic field components for each region in Fig. 1 can be found from their vector potentials (or Hertzian vectors),  $\vec{A}$  and  $\vec{F}$ , such as [22]

$$\vec{E}^{(n)} = -j \left\{ \omega \vec{A}^{(n)} - \frac{1}{\omega \mu_{(n)} \varepsilon_{(n)}} \nabla \left( \nabla \cdot \vec{A}^{(n)} \right) \right\} - \frac{1}{\varepsilon_{(n)}} \nabla \times \vec{F}^{(n)}, \quad (1)$$

$$\vec{H}^{(n)} = -j \left\{ \omega \vec{F}^{(n)} + \frac{1}{\omega \mu_{(n)} \varepsilon_{(n)}} \nabla \left( \nabla \cdot \vec{F}^{(n)} \right) \right\} + \frac{1}{\mu_{(n)}} \nabla \times \vec{A}^{(n)}, \quad (2)$$

where  $n = \text{I, II and III}$ ,  $\omega$  is the angular frequency, and  $\varepsilon_{(n)} = \varepsilon'_{(n)} - j\varepsilon''_{(n)}$  and  $\mu_{(n)} = \mu'_{(n)} - j\mu''_{(n)}$  are the complex permittivity and complex permeability of each region.

In the analysis, we assume that electromagnetic waves propagate to waveguide region II in  $-z$  direction with the dominant mode (TE <sup>$z$</sup> <sub>10</sub>) from region I. In addition, we assume that the sample has a flat surface over  $y$  axis at locations of  $x = L_1$  and  $x = L_1 + L$  and its surfaces are parallel to the left and right inner walls of the waveguide. Since TE <sup>$z$</sup> <sub>10</sub> mode has an electric field dependency in solely  $y$  direction, only the LSE <sup>$x$</sup>  modes will propagate through waveguide region II. For these modes, we can utilize  $\vec{A}^{(\text{II})} = 0$  and  $F_y^{(\text{II})} = F_z^{(\text{II})} = 0$  where the superscript 'II' in parenthesis denotes region II [22]. If we, respectively, denote  $F_{x01}^{(\text{II})}$ ,  $F_{x02}^{(\text{II})}$  and  $F_{xd}^{(\text{II})}$  for the  $x$ -components of the  $F^{(\text{II})}$  of the left and right air-filled and dielectric-filled portions in region II, the scalar wave equation (Helmholtz equation) for each portion in region II is given as

$$\nabla_t^2 F_{xm}^{(\text{II})} + [\gamma^2 + \kappa(x) \beta_0^2] F_{xm}^{(\text{II})} = 0, \quad m = 01, 02, d \quad (3)$$

where

$$\kappa(x) = \left\{ \begin{array}{ll} 1 & 0 \leq x \leq L_1, \quad L_1 + L \leq x \leq a \\ \varepsilon_r & L_1 \leq x \leq L_1 + L \end{array} \right\}. \quad (4)$$

Solutions for  $F_{xm}^{(\text{II})}$  which satisfies the Helmholtz equation in (3) are in the form [22]

$$F_{x01}^{(\text{II})} = C_1 \sin(\beta_{x0}x) \cos(\beta_{y0}y) e^{\gamma_{z0}z}, \quad 0 \leq x \leq L_1 \quad (5)$$

$$F_{x02}^{(\text{II})} = C_2 \sin(\beta_{x0}(a-x)) \cos(\beta_{y0}y) e^{\gamma_{z0}z}, \quad L_1 + L \leq x \leq a \quad (6)$$

$$F_{xd}^{(\text{II})} = C_3 \sin(\beta_{xd}(x - L_1 - L/2)) \cos(\beta_{yd}y) e^{\gamma_{zd}z}, \quad L_1 \leq x \leq L_1 + L \quad (7)$$

where  $C_1, C_2$  and  $C_3$  are complex or real constants;  $\beta_{x0}, \beta_{xd}, \beta_{y0}$  and  $\beta_{yd}$  are, respectively, the wave numbers of air-filled and dielectric-filled portions in  $x$  and  $y$  directions which will be determined by boundary conditions; and  $\gamma_{z0}$  and  $\gamma_{zd}$  are the propagation constants of air-filled and dielectric-filled portions in  $z$  direction. Applying boundary conditions (the continuation of electric and magnetic fields at air-dielectric interfaces), we obtain the following eigen equations

$$\beta_{y0} = \beta_{yd} = n\pi/b, \quad \gamma_{z0} = \gamma_{zd} = \gamma, \quad (8)$$

$$\gamma^2 = \beta_{xd}^2 + \beta_{y0}^2 - \epsilon_r \beta_0^2 = \beta_{x0}^2 + \beta_{y0}^2 - \beta_0^2 \Rightarrow \beta_{xd}^2 = \beta_{x0}^2 + (\epsilon_r - 1) \beta_0^2, \quad (9)$$

$$\begin{aligned} &\beta_{x0}^2 \tan(\beta_{xd}L) + \beta_{x0}\beta_{xd} (\tan(\beta_{x0}L_1) + \tan(\beta_{x0}L_2)) \\ & - \beta_{xd}^2 \tan(\beta_{xd}L) \tan(\beta_{x0}L_1) \tan(\beta_{x0}L_2) = 0 \end{aligned} \quad (10)$$

where  $n = 0, 1, 2, \dots$  and  $\beta_0$  is the wave number of electromagnetic waves propagating in an unbounded free-space region. The expressions in (8) comes from the fact that boundary conditions are satisfied at specific  $x$  values and are valid for all  $y$  and  $z$  values at the interfaces. Furthermore, the derivation of the eigen expression in (10) can be directly derived from the transverse-resonance method [24, 25].

In regions I and III, the  $LSE^x$  modes emerging from the region II will become evanescent modes and will die out drastically in a short distance away from the region II with no energy being carried out. It is important to note that this attenuation is not due to any energy losses; it simply results from the fact that the boundary conditions cannot be satisfied by any  $LSE^x$  modes in regions I and III [26]. Therefore, the normal mode of propagation in regions I and III will be similar to that of  $TE_{10}^z$ .

### 3. THE METHOD

#### 3.1. Mathematical Analysis

We will utilize propagation constant,  $\gamma$ , measurements at two locations of the sample inside the waveguide aperture to derive expressions for thickness-independent complex permittivity measurements of thin dielectric samples. From (10), for symmetric position of the sample into the waveguide, we have

$$\beta_{x0} \cot(\beta_{x0}(a - L)/2) = \beta_{xd} \tan(\beta_{xd}L/2) \quad (11)$$

$$\beta_{xd} \tan(\beta_{x0}(a - L)/2) + \beta_{x0} \tan(\beta_{xd}L/2) = 0 \quad (12)$$

where (11) and (12) correspond to symmetric and asymmetric modes which result in a short circuit and an open circuit at  $x = a/2$ , respectively.

For thin samples, one can assume that only the dominant mode in region II ( $\text{LSE}_{mn}^x = \text{LSE}_{10}^x$ ) will propagate. The frequency bandwidth for the dominant mode will be limited by the appearance of the first higher order mode  $\text{LSE}_{20}^x$ . The dependency of this bandwidth over sample thickness is analyzed in [27] and it was shown that, for a relative width of  $L/a < 0.25$ , the bandwidth in the partially filled waveguide as in Fig. 1 significantly increases. Therefore, we can assume that, for thin samples with lower dielectric permittivity values, only the  $\text{LSE}_{10}^x$  mode will propagate along  $z$  axis and the effects of higher order modes can be eliminated. As a result, we will only focus on symmetric modes.

For thin samples, we can assume that  $\beta_{xd}L \ll 1$ . This circumstance reduces (11) to [15]

$$\beta_{x0} \cot(\beta_{x0}(a-L)/2) \cong \beta_{xd}^2 L/2 = (\beta_{x0}^2 + (\varepsilon_r - 1)\beta_0^2) L/2. \quad (13)$$

It is clear from (13) that  $\varepsilon_r$  is a function of  $L$ . In this paper, in order to obtain  $\varepsilon_r$  with no information on  $L$ , together with (13), we utilize (10). For thin samples, the expression in (10) reduces to

$$(\beta_{xd}^2 \tan(\beta_{x0}L_1)\tan(\beta_{x0}L_2) - \beta_{x0}^2) L \cong \beta_{x0} (\tan(\beta_{x0}L_1) + \tan(\beta_{x0}L_2)). \quad (14)$$

Then, substituting  $L$  in (14) into (13), we obtain a metric function for  $\varepsilon_r$  extraction with no  $L$  dependence as

$$\begin{aligned} & \cot\left(\frac{\beta_{x0}}{2}\left(a - \frac{\beta_{x0}(\tan(\beta_{x0}L_1) + \tan(\beta_{x0}L_2))}{(\beta_{xd}^2 \tan(\beta_{x0}L_1)\tan(\beta_{x0}L_2) - \beta_{x0}^2)}\right)\right) \\ & (\beta_{xd}^2 \tan(\beta_{x0}L_1)\tan(\beta_{x0}L_2) - \beta_{x0}^2) \\ & \cong (\beta_{x0}^2 + (\varepsilon_r - 1)\beta_0^2) (\tan(\beta_{x0}L_1) + \tan(\beta_{x0}L_2))/2. \end{aligned} \quad (15)$$

It is important to point out that the advantage of the proposed method is that it increases the accuracy of  $\varepsilon_r$  measurement of the method in [17] since it needs the information on  $L_1$  and  $L_2$  instead of  $L$ . It is for sure that the accuracy of thickness measurement of a material drastically decreases with a decrease in its length.

### 3.2. Numerical Analysis

It is instructive to analyze the effect of sample shifting on the cutoff frequency and the propagation constant of the partially filled waveguide structure in Fig. 1. Use of perturbational techniques shows that the cutoff frequency for the structure in region II in Fig. 1 is between those of completely filled with the dielectric slab and of

completely filled with air [22]. The cutoff frequency of a completely filled waveguide section with  $LSE_{mn}^x$  modes can be found by

$$f_{c\ mn}^{TE^x} = \frac{c}{2\pi\sqrt{\varepsilon_g}}\sqrt{\left(\frac{m\pi}{a}\right)^2 + \left(\frac{n\pi}{b}\right)^2}, \quad m=1, 2, 3, \dots \quad n=0, 1, 2, \dots \quad (16)$$

where  $\varepsilon_g$  is the relative complex permittivity of the section completely filling the structure. Considering (16) and the information given above, we draw the dependency of cutoff frequencies over sample shift from the central of the guide ( $x = a/2$ ) in Fig. 2. In the analysis, we use the following test parameters:  $\varepsilon_r = 2.56$ ,  $L = 1$  mm,  $a = 22.86$  mm and  $b = 10.16$  mm.

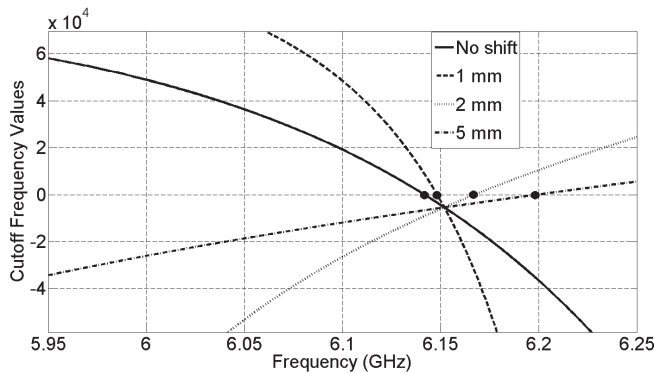


**Figure 2.** Dependency of cutoff frequencies, which are determined by the zero ordinate, over sample shift from the center ( $x = a/2$ ).

It is seen from Fig. 2 that cutoff frequencies are not much affected by the sample shift from the center ( $x = a/2$ ). Furthermore, it is noted that the cutoff frequency of the partially filled waveguide in Fig. 1 is near the one of empty waveguide section with the same propagation mode. This is because the sample is very thin.

In addition to evaluating the effect of sample shift on cutoff frequency, it is also important to monitor the impact of sample shift on propagation constant,  $\gamma$ . This analysis is important since it can demonstrate the sensitivity of the proposed method which depends on propagation constant measurements of the sample at two different locations. Fig. 3 demonstrates the dependency of propagation constants over sample shift from the center ( $x = a/2$ ) for the same test parameters used in drawing Fig. 2.

It is seen from Fig. 3 that larger sample shifting from the center results in separated propagation constant values, which in turn increase

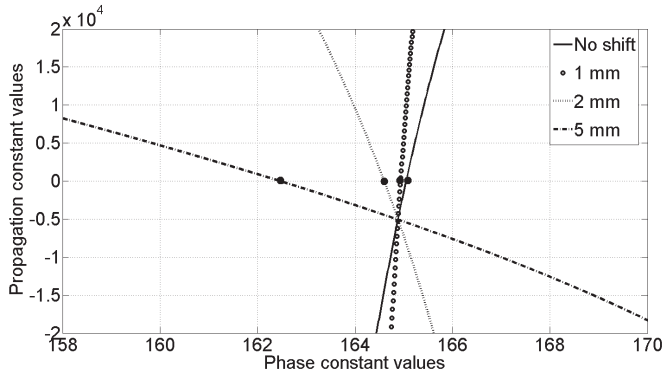


**Figure 3.** Dependency of propagation constant values, which are determined by the zero ordinate, over sample shift from the center ( $x = a/2$ ).

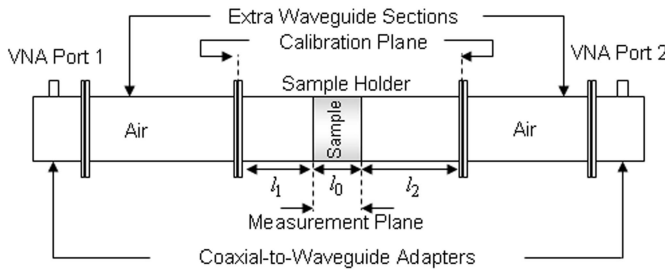


**Figure 4.** Measurement set-up.

the accuracy and performance of  $\epsilon_r$  measurement by our proposed method.

### 4. MEASUREMENT SET-UP

A general purpose waveguide measurement set-up is used for validation of the proposed method, as shown in Fig. 4. A HP8720C VNA is connected as a source and measurement equipment. It has a 1 Hz frequency resolution (with option 001) and 8 ppm (parts per million) frequency accuracy. The waveguide sections have a width of  $22.86 \pm 5\%$  mm ( $f_c \cong 6.555$  GHz). Two coax-to-waveguide adapters are used to connect the waveguide system to ports 1 and 2 of the VNA through flexible cables.

In Section 2, we assumed a single-mode transmission ( $LSE_{10}^x$ ) in region II in Fig. 1. This condition for empty and sample-filled

sections of the waveguide may not be consisted for samples with high permittivity values. In this case, higher-order modes may appear. Using two extra waveguide sections with lengths greater than  $2\lambda_0$  ( $\lambda_0$  is the free-space wavelength) between the sample holder and coaxial-to-waveguide adapters will eliminate not only higher-order modes such as LSE<sub>20</sub><sup>z</sup> in region II in Fig. 1 but also these evanescent modes in regions I and III in Fig. 1. This is because evanescent modes in regions I and III in Fig. 1 will die out drastically in a short distance away from region II and real measurements are performed at waveguide adapters. We use extra waveguide sections to eliminate any higher-order mode as shown in Fig. 4.

Measurements of propagation constants and then  $\varepsilon_r$  of samples are carried out as follows. First, forward and reverse transmission and reflection complex  $S$ -parameters are measured. Then, measurements are transformed from the calibration planes to measurement planes as shown in Fig. 4. Next, propagation constant is determined by

$$S_{11} = S_{11}^m e^{j2\beta_{z0}l_1}, \quad S_{22} = S_{22}^m e^{j2\beta_{z0}l_2}, \quad (17)$$

$$S_{21} = S_{21}^m e^{j\beta_{z0}(l_1+l_2)}, \quad S_{12} = S_{12}^m e^{j\beta_{z0}(l_1+l_2)}, \quad (18)$$

$$S_r^{av} = (S_{11} + S_{22})/2, \quad S_t^{av} = (S_{21} + S_{12})/2, \quad \beta_{z0} = \sqrt{(\omega/c)^2 - (\pi/a)^2}. \quad (19)$$

$$V_1 = S_t^{av} + S_r^{av}, \quad V_2 = S_t^{av} - S_r^{av}, \quad K = (1 - V_1V_2)/(V_1 - V_2), \quad (20)$$

$$\Gamma = K \pm \sqrt{K^2 - 1}, \quad T = (V_1 - \Gamma)/(1 - V_1\Gamma), \quad \gamma = -\ln(T)/l_0. \quad (21)$$

where  $S_{11}^m$ ,  $S_{21}^m$ ,  $S_{22}^m$  and  $S_{12}^m$  are, respectively, the forward and reverse reflection and transmission  $S$ -parameters;  $S_r^{av}$  and  $S_t^{av}$  are the averaged-out reflection and transmission  $S$ -parameters;  $l_1$ ,  $l_2$ , and  $l_0$  are, respectively, the distances between sample and terminals of the cell and the width of the sample in Fig. 4;  $\beta_{z0}$  is the phase constant (TE<sub>10</sub><sup>z</sup> mode) for the region between sample end surfaces and calibration planes;  $\Gamma$  and  $T$  are the first reflection and transmission coefficients of the sample.

Finally, utilizing the expressions in (17)–(21) and (15), the  $\varepsilon_r$  of a sample can be inverted. It should be pointed out that the derived expressions are not valid either for non-uniform cells [28, 29] or anisotropic materials [30].

## 5. MEASUREMENT RESULTS

We prepared some thin low-loss materials for validation of the proposed method and carried out measurements as discussed above. We followed the procedure discussed in Section 4 to measure the  $\varepsilon_r$  of a 2 mm

long Plexiglas sample. Since the accuracy of thickness-independent  $\varepsilon$  measurements by the proposed method depends on how accurately  $L_1$  and  $L_2$  are measured, we applied a simple procedure for their correct measurements as follows. We measured  $L_1$  and  $L_2$  by a micrometer at more than 10 locations between sample lateral surfaces and waveguide inner walls. Their averaged-out values are utilized in measurements of  $\varepsilon$  of thin materials. These measurements not only evaluate that each measurement of  $L_1$  and  $L_2$  at ten different locations is within the accuracy ranges, but also validate whether the assumption that the sample has a flat surface over  $y$  axis at locations of  $x = L_1$  and  $x = L_1 + L$  and its surfaces are parallel to the left and right inner walls of the waveguide in Fig. 1.

To ensure and increase the accuracy of measured propagation constant at a given asymmetric position of the sample inside its holder, we first switched the ends of the sample holder and then re-measured the propagation constant for this connection. Finally, we compared these constants. This procedure is similar to that used in calibration-independent measurements [31].

The thru-reflect-line (TRL) calibration technique is utilized before measurements [32]. We use a waveguide short and the shortest waveguide spacer (44.38 mm) in our lab for reflect and line standards, respectively. The line has a  $\pm 70^\circ$  maximum offset from  $90^\circ$  between 9.7 GHz and 11.7 GHz. After calibration, we apply time-domain gating to decrease post reflections, which may arise after the TRL calibration, and to obtain smoother complex scattering ( $S$ -) parameter measurements.

It is important to discuss on any mode coupling which may happen at the interface between calibration planes and the extra waveguide sections in Fig. 4 [33]. This is because the derivations presented in Sections 2 and 3 do not consider this coupling. To investigate the effect of this coupling, we measure amplitudes of reflection and transmission  $S$ -parameters for two connections: a) when extra waveguide sections are connected between the adapters and the sample holder (without the sample) and b) when the sample holder (without the sample) is directly connected to the adapters. If there is any mode coupling at the interface between the calibration planes and the extra waveguide sections, then it is expected that measured amplitudes of reflection and transmission  $S$ -parameters moderately change for the two connections. For example, Fig. 5 demonstrates the dependency of the amplitudes of  $S_{21}$  over X-band for these two measurement configurations.

It is seen from Fig. 5 that the measured amplitudes of  $S_{21}$  for these connections are approximately the same between 9.7 GHz and 11.7 GHz. This clearly verifies that the mode coupling, if any, is

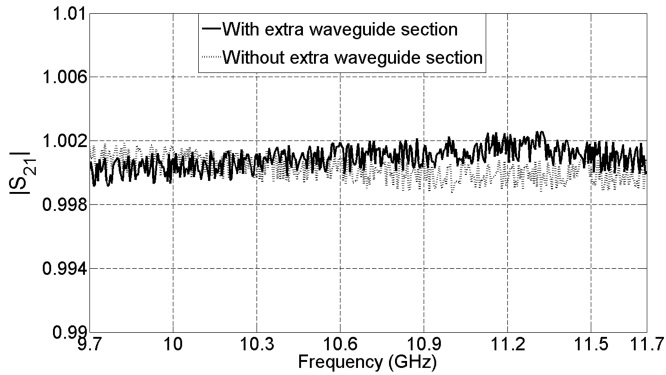


**Figure 5.** Measured  $S_{21}$  over 9.7–11.7 GHz for measuring any mode coupling from two measurement configurations.

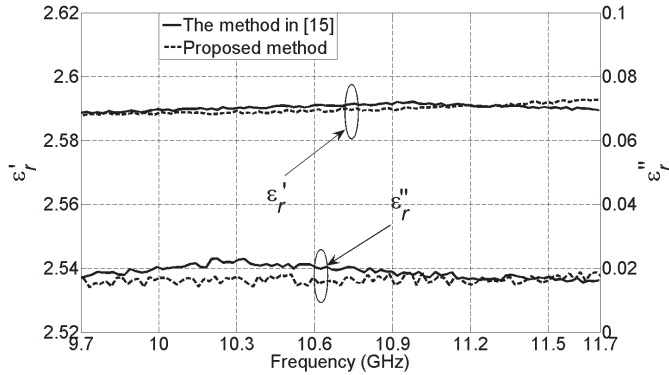


**Figure 6.** Measured  $\epsilon_r$  of a 2 mm long Plexiglas sample positioned longitudinally into the waveguide structure in Fig. 1 by the proposed method and by the one in [15].

negligible and the derivations given in Sections 2 and 3 can safely be applied for  $\epsilon_r$  measurement.

For validation of the proposed method, we arbitrarily located a 2 mm long Plexiglas sample into an X-band (8.2–12.4 GHz) waveguide aperture with  $a = 22.86$  mm. We then measured  $L_1$  and  $L_2$  as  $L_1 = 8.8 \pm 0.04$  mm and  $L_2 = 12.06 \pm 0.04$  mm by following the aforementioned procedure. For comparison of the accuracy of the proposed method, we also measured its  $\epsilon_r$  by the method in [15]. The results are plotted in Fig. 6.

It is seen from Fig. 6 that the extracted  $\epsilon_r$  by the proposed method

is in good agreement with that by the method in [15]. In addition, it is seen from Fig. 6 that our proposed method determines a  $\varepsilon_r$  which is very close to the reference data ( $\varepsilon_r = 2.59 - j0.0174$ ) available in the literature [34]. It is because our proposed method utilizes measurements of  $L_1$  and  $L_2$  in Fig. 1 instead of direct measurement of  $L$ .

It is noted that the maximum and minimum lengths of the sample that the proposed method can be applied depend on how much  $\beta_{xd}L$  is smaller than one. It should be pointed out that, assuming that the length uncertainty is kept constant, the accuracy of measurements by the proposed method increases for samples with higher permittivity values since the relative measurement error in  $\varepsilon_r$  decreases.

## 6. CONCLUSION

A microwave method has been proposed for accurate measurement of complex permittivity of thin materials partially filling the waveguide aperture. The proposed method utilizes scattering parameter measurements at two locations of the sample (the one at the center and the other one far away from the center) inside its holder. We have derived a useful expression for accurate  $\varepsilon_r$  inversion of these materials and validated the proposed method by  $\varepsilon_r$  measurements of a thin Plexiglas sample at X-band.

## ACKNOWLEDGMENT

U. C. Hasar (Mehmetcik) would like to thank TUBITAK (The Scientific and Technological Research Council of Turkey) Münir Birsal National Doctorate Scholarship and YOK (The Higher Education Council of Turkey) Doctorate Scholarship for supporting his studies.

## REFERENCES

1. Chen, L. F., C. K. Ong, C. P. Neo, et al., *Microwave Electronics: Measurement and Materials Characterization*, John Wiley & Sons, West Sussex, England, 2004.
2. Nyfors, E., "Industrial microwave sensors — A review," *Subsurface Sensing Tech. and Appl.*, Vol. 1, 23–43, 2000.
3. Hebeish, A. A., M. A. Elgamel, R. A. Abdelhady, et al., "Factors affecting the performance of the radar absorbant textile materials of different types and structures," *Progress In Electromagnetics Research B*, Vol. 3, 219–226, 2008.

4. Zhang, H., S. Y. Tan, and H. S. Tan, "An improved method for microwave nondestructive dielectric measurement of layered media," *Progress In Electromagnetics Research B*, Vol. 10, 145–161, 2008.
5. Li, E., Z.-P. Nie, G. Guo, Q. Zhang, Z. Li, and F. He, "Broadband measurements of dielectric properties of low-loss materials at high temperatures using circular cavity method," *Progress In Electromagnetics Research*, PIER 92, 103–120, 2009.
6. Williams, T. C., M. A. Stuchly, and P. Saville, "Modified transmission-reflection method for measuring constitutive parameters of thin flexible high-loss materials," *IEEE Trans. Microw. Theory Tech.*, Vol. 51, 1560–1566, 2003.
7. Hasar, U. C., "Thickness-independent automated constitutive parameters extraction of thin solid and liquid materials from waveguide measurements," *Progress In Electromagnetics Research*, PIER 92, 17–32, 2009.
8. Weir, W. B., "Automatic measurement of complex dielectric constant and permeability at microwave frequencies," *Proc. IEEE*, Vol. 62, 33–36, 1974.
9. Nicolson, A. M. and G. Ross, "Measurement of the intrinsic properties of materials by time-domain techniques," *IEEE Trans. Instrum. Meas.*, Vol. 19, 377–382, 1970.
10. Hasar, U. C., "An accurate complex permittivity method for thin dielectric materials," *Progress In Electromagnetics Research*, PIER 91, 123–138, 2009.
11. Hasar, U. C., "Two novel amplitude-only methods for complex permittivity determination of medium- and low-loss materials," *Meas. Sci. Technol.*, Vol. 19, 055706–055715, 2008.
12. Hasar, U. C., "A fast and accurate amplitude-only transmission-reflection method for complex permittivity determination of lossy materials," *IEEE Trans. Microw. Theory Tech.*, Vol. 56, 2129–2135, 2008.
13. Hasar, U. C. and C. R. Westgate, "A broadband and stable method for unique complex permittivity determination of low-loss materials," *IEEE Trans. Microw. Theory Tech.*, Vol. 57, 471–477, 2009.
14. Catala-Civera, J. M., A. J. Canos, F. L. Penaranda-Foix, and E. de los Reyes Davo, "Accurate determination of the complex permittivity of materials with transmission reflection measurements in partially filled rectangular waveguides," *IEEE Trans. Microw. Theory Tech.*, Vol. 51, 16–24, 2003.

15. Chung, B. K., "A convenient method for complex permittivity measurements of thin materials at microwave frequencies," *J. Physics D: Appl. Phys.*, Vol. 39, 1926–1931, 2006.
16. Akhtar, J. M., L. E. Feher, and M. Thumm, "Noninvasive procedure for measuring the complex permittivity of resins, catalysts, and other liquids using a partially filled rectangular waveguide structure," *IEEE Trans. Microw. Theory Tech.*, Vol. 57, 458–470, 2009.
17. Chung, B.-K., "Dielectric constant measurement for thin material at microwave frequencies," *Progress In Electromagnetics Research*, PIER 75, 239–252, 2007.
18. Murata, K., A. Hanawa, and R. Nozaki, "Broadband complex permittivity measurement techniques of materials with thin configuration at microwave frequencies," *J. Applied Phys.*, Vol. 98, 084107-1–084107-08, 2005.
19. Pitarch, J., M. Contelles-Cervera, F. L. Penaranda-Foix, and J. M. Catala-Civera, "Determination of the permittivity and permeability for waveguides partially loaded with isotropic samples," *Meas. Sci. Technol.*, Vol. 17, 145–152, 2006.
20. Olmi, R., M. Tedesco, C. Riminesi, et al., "Thickness-independent measurement of the permittivity of thin samples in the X band," *Meas. Sci. Technol.*, Vol. 13, 503–509, 2002.
21. Baker-Jarvis, J., M. D. Janezic, P. D. Domich, et al., "Analysis of an open-ended coaxial probe with lift-off for nondestructive testing," *IEEE Trans. Instrum. Meas.*, Vol. 43, 711–718, 1994.
22. Balanis, C. A., *Advanced Engineering Electromagnetics*, John Wiley & Sons, New Jersey, NJ, 1989.
23. Harrington, R. F., *Time-Harmonic Electromagnetic Fields*, John Wiley & Sons and IEEE Press, New York, NY, 2001.
24. Collin, R. E., *Field Theory of Guided Waves*, IEEE Press, New York, NY, 1991.
25. Marcuvitz, N., *Waveguide Handbook*, McGraw-Hill, New York, NY, 1951.
26. Inan, U. S. and A. S. Inan, *Electromagnetic Waves*, Prentice Hall, New Jersey, NJ, 2000.
27. Vartanian, P. H., W. P. Ayres, and A. L. Helgesson, "Propagation in dielectric slab loaded rectangular waveguide," *IRE Trans. Microw. Theory Tech.*, Vol. 5, 215–222, 1958.
28. Challa, R. K., D. Kajfez, J. R. Gladden, and A. Z. Elsherbeni, "Permittivity measurement with a non-standard waveguide by using TRL calibration and fractional linear data fitting," *Progress*

- In Electromagnetics Research B*, Vol. 2, 1–13, 2008.
29. Khalaj-Amirhosseini, K., “Closed form solutions for nonuniform transmission lines,” *Progress In Electromagnetics Research B*, Vol. 2, 243–258, 2008.
  30. Valagiannopoulos, C. A., “On measuring the permittivity tensor of an anisotropic material from the transmission coefficients,” *Progress In Electromagnetics Research B*, Vol. 9, 105–116, 2008.
  31. Hasar, U. C. and O. E. Inan, “Elimination of the dependency of the calibration plane and the sample thickness from complex permittivity measurements of thin materials,” *Microw. Opt. Technol. Lett.*, Vol. 51, 1642–1646, 2009.
  32. Engen, G. F. and C. A. Hoer, “‘Thru-reflect-line’: An improved technique for calibrating the dual six-port automatic network analyzer,” *IEEE Trans. Microw. Theory Tech.*, Vol. 27, 987–993, 1979.
  33. Hasar, U. C., “Simple calibration plane-invariant method for complex permittivity determination of dispersive and nondispersive low-loss materials,” *IET Microw. Antennas Propagat.*, Vol. 3, 630–637, 2009.
  34. Von Hippel, A. R., *Dielectric Materials and Applications*, John Wiley & Sons, New York, NY, 1954.